JOURNAL OF PROPULSION AND POWER
Vol. 17, No. 1, January–February 2001

Model of Particulate Interaction with Plasma in a Teflon Pulsed Plasma Thruster

Michael Keidar* and Iain D. Boyd†
University of Michigan, Ann Arbor, Michigan 48109
and
Isak I. Beilis‡
Tel Aviv University, Tel Aviv 69978, Israel

The presence of particulates [referred to as macroparticles (MPs)] in the plume of a pulsed plasma thruster (PPT) may affect interaction with the spacecraft. Possible particulate related effects depend on particulate properties. The MPs emitted into the plasma during the discharge may be charged, accelerated, and heated by the ion, electron, and neutral fluxes depending on the MP residual time. Different aspects of MP–plasma interaction in the experimentally observed range of MP radii (0.1–100 μm) are analyzed. It is found that the charging time is smaller whereas the steady-state potential is larger in the case of a large MP. A 1-μm MP is found to have a charge of about 10^5 electrons in the case of an electron density of about 10^{23} m^{-3}. The two primary forces acting on the MP in the PPT discharge are a drag force due to collision with neutral atoms and ions and an electric force due to the presence of the electric field in the current carrying plasma. The calculation of the MP velocity shows that the maximum possible velocity of a 1-μm MP is about 230 m/s, which is close to that estimated experimentally. Only small MPs ($\sim$ 0.1 μm) can be entrained by the plasma jet, whereas large MPs are generally slower and flow substantially behind the plasma jet. MP temperature and decomposition rates are calculated by solving a heat balance equation. It is found that small MPs (<1 μm) may completely decompose during a 1-μs pulse.

Nomenclature

C	=	specific heat
C_s	=	sound speed
E	=	electric field
F_d	=	total drag force
g	=	Teflon® ablation rate
I	=	discharge current
$J_e(r)$	=	electron current density in the sheath around microparticle (MP)
J_{e0}	=	electron thermal flux at the plasma–sheath interface
$J_i(r)$	=	ion current density in the sheath around MP
J_{i0}	=	ion flux in the absence of a field at the plasma–sheath interface
j	=	current density
L	=	cavity length
L_D	=	Debye length
M_p	=	MP mass
m_a	=	atom mass
N	=	plasma density at the plasma–sheath interface
N_a	=	plasma density near the anode, that is, where $z = 0$
Nu	=	Nusselt number
n	=	plasma density normalized by N_a
P_0	=	equilibrium pressure
Q_d	=	cooling rate due to decomposition of material
$Q_{i,e}$	=	heat rate due to ion and electron flux
Q_n	=	neutral atom heat flux
Q_p	=	MP charge
Q_r	=	radiation cooling rate
R_p	=	MP radius
R_{p0}	=	initial MP radius
r_a	=	radius of cavity
T	=	neutral gas temperature
T_e	=	electron temperature
T_i	=	ion temperature
T_p	=	MP temperature
U_p	=	MP potential with respect to the plasma
U_s	=	potential drop in the near spacecraft surface sheath
V	=	plasma velocity
V_d	=	MP ablation rate
V_p	=	MP velocity
V_{pn}	=	normal component of the MP velocity
v	=	plasma velocity normalized by the sound speed
z	=	coordinate in the axial direction normalized by cavity length
α	=	heat transfer coefficient
ΔH	=	ablation heat
ΔT	=	temperature difference between the plasma and the MP
Δt	=	residual time of MP in discharge
ε	=	dielectric permittivity of Teflon®
ε_0	=	permittivity of vacuum
λ_C	=	mean free path
ξ	=	particle emissivity
ρ	=	specific density
σ	=	plasma conductivity
σ_r	=	Stefan–Boltzmann constant
τ	=	dimensionless time, L_D/C_s
ϕ	=	normalized MP potential, eU_p/kT_e

Received 10 May 1999; revision received 17 January 2000; accepted for publication 25 February 2000.

*Associate Professor, Department of Aerospace Engineering. Senior Member AIAA.
†Research Fellow, Department of Aerospace Engineering. Member AIAA.
‡Professor, Electrical Discharge and Plasma Laboratory, P.O. Box 39040.

I. Introduction

THE pulsed plasma thruster (PPT) has been reconsidered recently as an attractive spacecraft propulsion option.[1,2] This has happened mainly due to a greater emphasis being placed on the development of satellites with reduced size for many applications. PPTs are expected to provide exact impulse bits to be used for accurate attitude control. The principal advantage of PPTs is their simple design, which provides high reliability. In particular, the higher reliability of the PPT is achieved through the use of solid propellant, which eliminates design and operation complexity connected with using liquid and gas propellants.

Unfortunately, the PPT has a very poor performance characteristic. For instance, a flight-qualified PPT design had an efficiency of about 8% (Ref. 3). One of the factors leading to low efficiency is the late neutral ablation.[4] Another factor that may significantly reduce the efficiency is the particulate emission. Estimates have shown that the particulate emission consumes about 40% of the total propellant mass, albeit contributing only 1% to the total thrust.[5]

Particulates, sometimes referred to as macroparticles (MPs), are emitted during the pulse and may interact with the surrounding plasma. Various experimental and theoretical aspects of MP interaction with plasma have been studied in different systems such as plasma assisted chemical vapor deposition,[6] plasma etching,[7] rf and glow discharge,[8,9] cathodic vacuum arc deposition,[10,11] and in-space plasma.[12] The MPs are subjected to charging, heating, and momentum transfer.[6–12] It may be concluded that in spite of many common features of MP–plasma interaction, the MP charge, velocity, and temperature depend on properties of the plasma and MP related to each specific system. Recently, results for the MP size distribution in a PPT have been presented by Spanjers et al.[5] Particulates were observed to have characteristic diameters ranging from about 0.1 μm to over 100 μm. The PPT plasma has a weak degree of ionization.[1] Thus, one can expect an important role of the neutral component in the momentum and energy transfer to MPs. No analyses of MP interaction with the PPT plasma have been reported previously. The present work has the primary objective of removing this deficiency by analyses of different aspects of MP behavior of a PPT, such as charging, acceleration, heating, and decomposition. This work will provide additional information about MPs to help mission planners in estimating the particulate contamination potential.

II. Model of MP–Plasma Interaction

In the present section we will develop the model of MP interaction with plasma, including MP charging, transport, and heating in a pulsed discharge. As a working example, we will concentrate on a specific type of PPT, developed at the University of Illinois, the so-called PPT-4 (Ref. 1). This PPT has a coaxial configuration in which Teflon® is ablated from a cylindrical cavity sitting in front of the central electrode of 6-mm diam and an annular electrode of 43-mm diam. The two electrodes are connected with a 30-deg half-angle nozzle. The typical PPT-4 pulse duration is about 10 μs with a current peak of about 8 kA. The main physical process in this type of thruster occurs in the Teflon cavity. Rapid heating of a thin dielectric surface layer leads to decomposition of the material of the wall. As a result of heating, decomposition, and partial ionization of the decomposition products, the total number of particles increases in the cavity.

At the same time, nonuniformities in the discharge distribution across the Teflon surface may cause overheating followed by phase change of propellant.[1] High plasma pressure in the PPT channel may lead to Teflon MP generation. However, the mechanism of such MP generation from the propellant is not understood sufficiently. Another possible source of MPs is the spot attachment at electrodes that is a typical phenomenon in the early stages of discharge.[13] Several scenarios leading to particle generation from the electrodes are possible: action of the plasma pressure on the liquid pool in the quasi-steady regime may form droplets, similar to that occurring in the vacuum arc cathode spot[14]; growth of the perturbation of the liquid surface due to the Rayleigh–Taylor instability may result in liquid jet fragmentation and small droplet generation, as it occurs in liquid-metal ion sources[15]; solid-particle generation due to a wave of thermoelastic stresses may also be caused by local overheating.[16]

In the experiment, basically two populations of MPs were found.[5] One population of MPs is characterized by a diameter less than 1 μm and by a spherical shape. It was concluded that these MPs come from the steel PPT electrodes[5] due to discharge attachment. The second population has a more random shape and size with maximal size up to 200 μm. The second population is concluded to be originated from the Teflon propellant.[5] In PPT-4, where copper electrodes were used, tracks of discharge attachment at the electrodes were not observed, as was noted in a private communication with R. L. Burton. However, Teflon macroparticles may still be generated that have a significant effect on propellant losses. Thus, as we consider the PPT-4 configuration in the present paper, we will concentrate on these MPs.

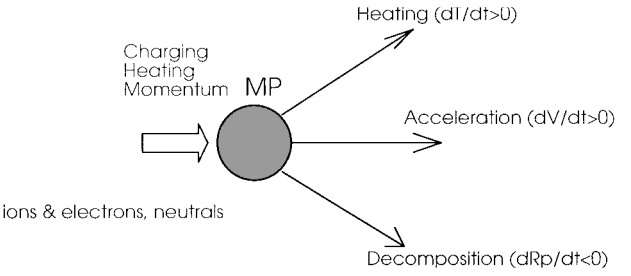

Fig. 1 Schematic presentation of MP–plasma interaction.

The MPs emitted into the plasma during the discharge may be charged, accelerated, and heated by the ion, electron, and neutral fluxes, depending on the MP residual time. It is assumed in the model that the MP may be emitted at any point of time during to the discharge pulse. This implies that MPs generated at the later stage of discharge will have less time for interaction with plasma. The scheme of MP–plasma interaction is shown in Fig. 1. The present model is based on the assumption that during the MP flight the plasma parameters do not change significantly, that is, the following condition is fulfilled: $V_p \Delta t \ll (\partial \ell n X/\partial z)^{-1}$, where X is any of the plasma parameters (velocity, density, and temperature). This model of plasma–MP interaction is approximation to the more complex reality in which plasma parameters vary during the MP residual time. In the present model, we will analyze the plasma–MP interaction having plasma density and velocity that lie in the range of their possible variation during the discharge pulse, as free parameters of the problem.

A. Quasi-Steady-State Plasma Model

The main features of the electrical discharge in the dielectric cavity include joule heating of the plasma, heat transfer to the Teflon, decomposition followed by ionization, and acceleration of the plasma up to the sound speed at the cavity exit. In this section, we will present a simple quasi-stationary model of the plasma flow in the Teflon cavity. A quasi-steady-state approach to the PPT flow has numerous limitations.[17] It requires that the propellant ablation must supply material to the discharge chamber in times shorter than the characteristic flow convection time, which, in turn, should be less than the characteristic time of discharge parameter variation. However, this approach may provide some useful information about the possible range of density in the discharge chamber and the spatial plasma density and velocity distribution along the cavity length. In the present model the plasma velocity and density will be used in the MP–plasma interaction model as parameters.

We apply a one-dimensional hydrodynamic model for the plasma under the assumption that the Teflon evaporates uniformly. Products of Teflon evaporation are partially ionized in the cavity. Partially ionized plasma conducts the current, which is carried in the direction parallel to the plasma flow. Therefore, for simplicity, we omit effects connected with electric and self-magnetic fields. Partially ionized plasma accelerates in the axial direction due to the pressure gradient and achieves the sound speed at the cavity exit plane.[18] Note that this is a dominant acceleration mechanism in the electrothermal PPT-4 device, whereas traditional PPT has predominant electromagnetic acceleration mechanism. Teflon evaporation is the origin of the source term in the mass conservation equation. In this case, the governing equations in dimensionless form are

$$\frac{dv}{dz} = \frac{\beta}{n(1-v^2)} \tag{1}$$

$$\frac{dn}{dz} = -\frac{n\,dv}{v\,dz} + \frac{\beta}{v} \tag{2}$$

where $\beta = g/(N_a C_s m_a \pi r_a^2)$ and $C_s = ([kT_e + kT_i]/m_i)^{0.5}$. The following boundary conditions are used for Eqs. (1) and (2): $n(z = 0) = 1$ and $dv/dz = 0$.

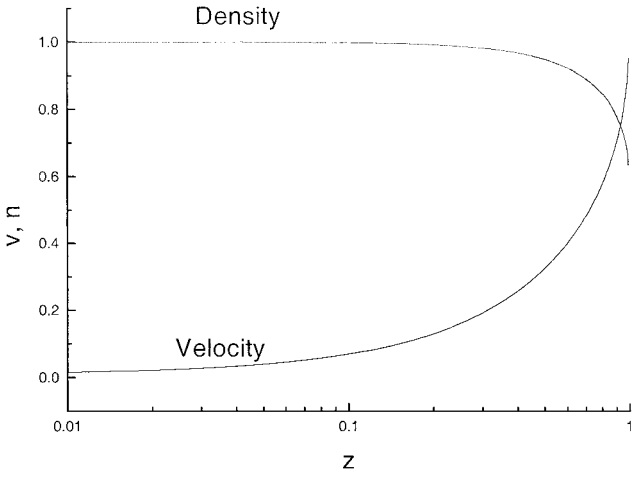

Fig. 2 Plasma density and velocity spatial distribution in the cavity, $\beta = 0.6$.

The plasma density and velocity distribution are shown in Fig. 2. Note that the plasma is significantly accelerated toward the cavity exit. Burton et al. obtained similar flowfield development in a liquid-injected capillary discharge[19] when the plasma flow approaches steady-state conditions. Taking into account that the plasma velocity should be sonic at the exit ($z = 1$), it is found that $\beta = 0.6$. In one PPT-4 design it was measured that the ablation rate is about 30 μg per 10-μs pulse.[20] One can estimate that the plasma density near the central electrode should be $\sim 10^{24}$ m^{-3} using this experimental value for g. Note, however, that the aforementioned estimated number density of the plasma in the cavity represents the low limit. This is because it was assumed that, in the framework of a quasi-steady-state model, the characteristic time is equal simply to the pulse duration. Under the assumption that the characteristic discharge time is about the acoustic time (L/C_s, which is typically a few microseconds) the plasma density near the central electrode may be substantially higher (up to an order of magnitude) than the preceding estimation.

B. MP Charging

An experimental investigation of the MP size distribution showed a variation from 0.1 up to 100 μm (Ref. 5). It was also found that some MPs have a spherical shape, whereas generally MPs have a rather random shape distribution.[5] To make it possible to develop a model quantitatively, we will assume that all MPs have a spherical shape with radii in the experimentally observed range. Under the typical conditions of PPT-4 operation, the electron density in the cavity during the pulse is about 10^{21}–10^{24} m^{-3}, which corresponds to a debye length of about 10^{-6}–10^{-7} m. It is known that the thickness of the sheath around a MP is about the Debye length.[21,22] Therefore, one can see that there are basically two cases: small MPs for which the Debye length is less than or about the MP radius, and large MPs for which the Debye length is much less than the MP radius. These two cases may be handled using different approaches for modeling the charging process. The second case is more straightforward and corresponds to that of a plane probe. The MP charging in the first case was developed in detail in Ref. 22.

In both cases, the MP charging process is modeled with the aid of the following assumptions: 1) The plasma consists of two species of charged particles. For PPT-4 conditions, thermal equilibrium between all species is achieved and, therefore, we assume that $T = T_e = T_i$. 2) The plasma jet flow is not substantially obstructed in the sheath around the MP, and, thus, spherical symmetry of the plasma density relative to the MP is assumed. 3) Self-magnetic field effects are neglected because PPT-4 has predominantly electrothermal acceleration mechanism.

The kinetics of the MP charging is controlled by the ion and electron fluxes to the MP, which depend on the potential distribution in the sheath. Using Maxwell's equation and assumption 3, the electric field $E(r)$ changes with time according to the relation

$$\varepsilon \frac{\partial E(r)}{\partial t} = -[J_i(r) + J_e(r)] \tag{3}$$

The time derivative of the electric field is a function of the radius r. An estimation indicated[22] that the characteristic time for the electric field to reach steady state decreases with radius and has its maximum value at the MP surface, that is, where $r = R_p$. Thus, Eq. (3) will be solved at the radius R_p. The electron and ion current densities are required to solve Eq. (3). The electron current density is calculated according to the following relation:

$$J_e = J_{e0} \exp(-eU_p/kT_e) \tag{4}$$

The ion current density depends on the ratio of Debye length to the MP radius and, thus, will be different for small and large MPs.

1. *Small MPs*

This case corresponds to the low limit of the measured MP size distribution function. In the case of a spherical sheath around an MP and $L_D > R_p$, the ion flux may be calculated using the orbital motion limit[23,24]:

$$J_i = J_{i0}(1 + eU_p/kT_i) \tag{5}$$

This expression is exact for an infinite L_D/R_p ratio. By considering different ion trajectories around the MP, it is possible to calculate the ion flux for a finite L_D/R_p ratio. An influence of this effect was examined in detail in Ref. 22.

In the general case, the capacitance of the MP in the plasma is given by $C = Q_p/U_p = 4\pi R_p \varepsilon_0 G(R_p/L_D)$. The function $G(R_p/L_D)$ is presented in Ref. 22, and, for the case $R_p/L_D \approx 1$, this function is $G(R_p/L_D) \approx 1.8$, whereas in the orbital motion limit this function is equal to 1.

When we take into account the preceding expression for MP capacitance and combine Eqs. (3–5), the kinetics of MP charging may be described by the following dimensionless equation (in the orbital motion limit):

$$\frac{\mathrm{d}\phi}{\mathrm{d}\tau} = \frac{R_p}{L_D}\frac{1}{\sqrt{2\pi}}\left(1 + \phi - \sqrt{\frac{m_i}{m_e}}e^{-\phi}\right) \tag{6}$$

2. *Large MPs*

In this case, the sheath model near the planar electrode can be used. Because in the cavity the plasma velocity is less than the sound speed (see Sec. II.A), the ion flux can be calculated from the Bohm expression[25]:

$$J_i = 0.4eNC_s \tag{7}$$

The capacitance in this case reads[26]

$$C = 4\pi R_p^2 \varepsilon_0 (1/R_p + 1/L_D) \sim 4\pi \varepsilon_0 \left(R^2 \big/ L_D\right) \tag{8}$$

When we take into account the expression for MP capacitance, the kinetics of MP charging may be described by the following dimensionless equation:

$$\frac{\mathrm{d}\phi}{\mathrm{d}\tau} = \left(0.4 - \sqrt{\frac{m_i}{2\pi m_e}}e^{-\phi}\right) \tag{9}$$

The time variation of the dimensionless MP potential is shown in Fig. 3 for two limiting cases of $R_p/L_D \gg 1$ and $R_p/L_D \ll 1$. Note that the charging time is smaller, whereas the steady-state potential is larger in the case $R_p/L_D \gg 1$. The steady-state potential increases from about 3.5 in the case of $R_p/L_D \ll 1$ up to about 5 in the case of $R_p/L_D \gg 1$. All possible cases realized in a typical PPT are placed between the limits of these two curves. Thus, in the PPT plasma with $T = 2$ eV, MP has a negative potential of about $-(7 \div 10)$ V with respect to the plasma.

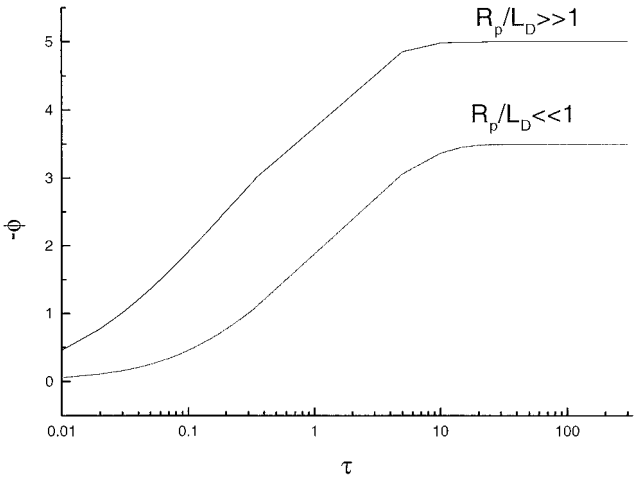

Fig. 3 Temporal behavior of dimensionless MP potential with R_p/L_D as a parameter.

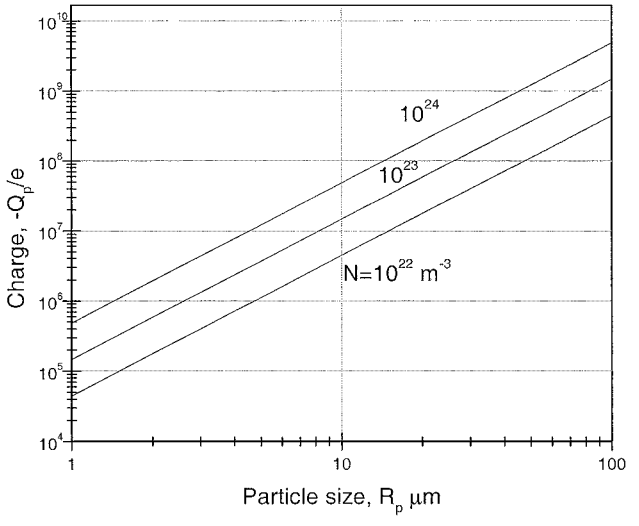

Fig. 4 MP charge dependence on the radius with electron density as a parameter, T_e = 1.5 eV.

3. MP Charge

To calculate possible values of the charge accumulated on the MP, we will convert from the dimensionless parameters. The MP charge (in the large MP limit) may be connected with the dimensionless potential as follows:

$$Q_p = 4\pi R_p^2 L_D N \phi \tag{10a}$$

In the small MP limit, the corresponding expression for the MP charge reads

$$Q_p = 4\pi \varepsilon_0 R_p \phi k T_e / e \tag{10b}$$

The calculated steady-state MP charge as a function of MP radius is shown in Fig. 4 with electron density as a parameter for the large MP limit ($R_p > 1$ μm). Note that the 1-μm MP has a charge of about 10^5 electrons in the case of $N = 10^{23}$ m^{-3}. One can see that, in this case, MP charge increases with electron density unlike the other case (small MP with $R_p < 1$ μm) when Q_p is independent of the plasma density. In the latter case, the MP charge is a linear function of R_p and can be estimated as $Q_p = 2.4 \cdot 10^3 \times R_p$ (micrometers) where Q_p is in electrons.

C. Momentum Transfer

There are two primary forces acting on the MP in the PPT discharge: 1) a drag force due to collision with neutral atoms and ions and 2) a force due to the presence of the electric field in a current carrying plasma. To predict the MP velocity, we simply integrate the equation of motion from some starting point. We assumed that MPs have zero initial velocity. Given the solution for plasma density and velocity distribution in the cavity, we evaluate the forces that act on an individual MP. The equation of motion of an individual MP may be written as

$$\frac{\mathrm{d}(M_p V_p)}{\mathrm{d}t} = F_d + Q_p E \tag{11}$$

The mass M_p of the MP traveling in the plasma may be changed as a result of MP ablation (see next section).

The first term is the total drag force and the second term is the electric force, which depends on the electric field in the plasma and the MP charge. An average electric field E in the plasma may be calculated from Ohm's law for known current density j, namely, $E = j/\sigma$. We will consider a diffuse discharge on the anode and, therefore, $j = I/\pi r_a^2$. The current density was estimated at the current peak of about 8 kA and plasma conductivity was calculated for electron temperature of about 2 eV (see Ref. 20).

In partially ionized plasmas, there are coulomb collisions of the MP with ions because the MP is charged. These collisions contribute to the drag and may result in a force called ion drag.[27] In low-density plasmas with large ratio of Debye length to MP radius (small MPs, see preceding section), it was found that the momentum transfer due to ions that are collected by a MP cross section is much less than that due to ions scattered but not collected.[21] Note that if the Debye length is much less than or about the MP size (large MPs), the momentum transfer is determined by the MP cross section.[28] In general, the neutral drag force is also determined by the MP cross section. Analyses of the MP size distribution and range of possible plasma densities (10^{21}–10^{24} m^{-3}) shows that both free molecular and continuum regimes for the drag force can be realized.

1. Small MP (Free Molecular Regime)

In the free molecular regime, that is, $R_p \ll \lambda_C$, the drag force can be written as[29]

$$F_d = \left(\sqrt{\pi}\rho R_p^2/2\beta\right)\left\{[s + (1/2s)\exp(-s^2)] + (s^2 + 1 - 1/4s^2)\sqrt{\pi}\,\mathrm{erf}(s)\right\} \tag{12}$$

where $\beta = m/2kT$ and $s = 2V_p/[\sqrt{(\pi)}(V - V_p)]$.

2. Large MP (Continuum Regime)

In this case the drag force that acts on the isolated MP placed into a plasma moving with velocity V is determined by the expression[30,31]

$$F_d = C_D \pi R_p^2 \rho (V - V_p)^2/2 \tag{13}$$

where C_D is the drag coefficient that depends on the Reynolds number. For instance, in the case of $Re \le 1$, coefficient $C_D = 24.8/Re$ (Refs. 30 and 31). Estimation shows that in the PPT plasma, the Reynolds number is about 10^{-3} V, where V is the plasma velocity in meters per second.

The calculation of the MP velocity in the continuum regime as a function of time with normalized plasma velocity as a parameter is plotted in Fig. 5a for the case $R_p = 1$ μm. Note that the maximum possible MP velocity is about 230 m/s. In experiments it was found that some MPs have a velocity of about 200 m/s (Ref. 5). Smaller MPs may have a larger velocity as shown in Fig. 5b for the case of $R_p = 0.1$ μm, calculated in the free molecular regime. One can see that the MP velocity depends on the residual time in the discharge. Thus, those MPs generated toward the end of the pulse are expected to have a smaller velocity.

The ratio of MP velocity to the plasma velocity dependence on the MP radius is shown in Fig. 6 with plasma density as a parameter. These calculationsare performed for the case of MP residual time

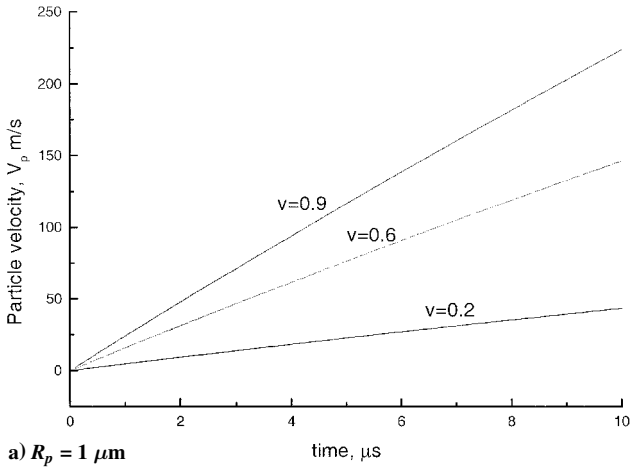

a) $R_p = 1$ μm

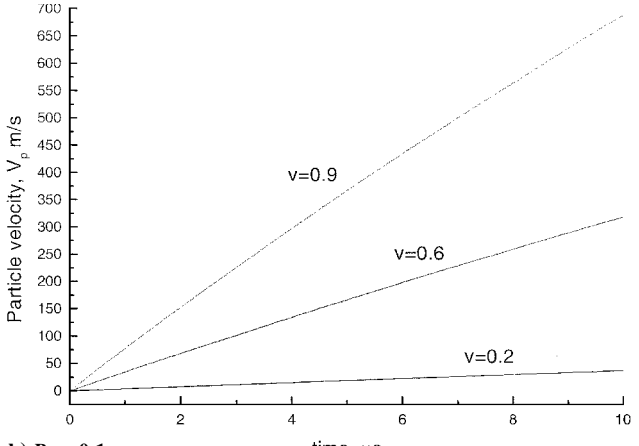

b) $R_p = 0.1$ μm

Fig. 5 Temporal behavior of the MP velocity with dimensionless plasma velocity as a parameter, $T_e = 1.5$ eV and $N = 10^{23}$ m^{-3}.

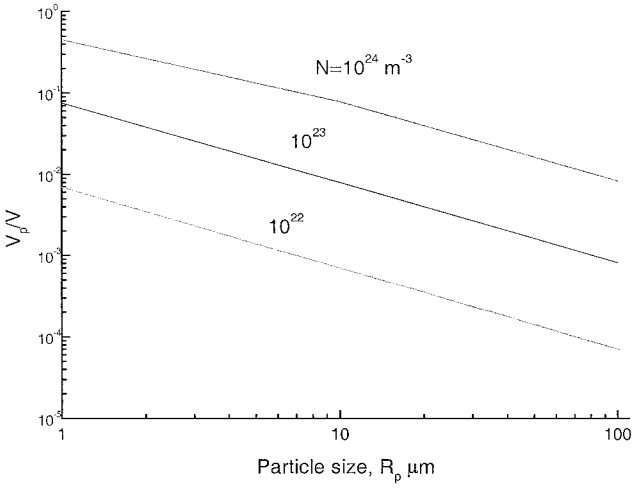

Fig. 6 Normalized MP velocity dependence on the MP radius with plasma density as a parameter, $T_e = 1.5$ eV and $\Delta t = 10$ μs.

equal to the discharge pulse, that is, for $t = 10$ μs. One can see that small MPs in the dense plasma can approach the plasma velocity and can be entrained by the plasma jet. However, the large MPs are generally slower and flow substantially behind the plasma jet.

Note that, due to ablation, the MP radius decreases in the course of interaction with the plasma, and, thus, MP–plasma interaction may change from initially continuum to free molecular. An effect of MP ablation is considered in the next section.

D. Heat Transfer

As the particle moves through the plasma, it is heated by neutral, electron, and ion fluxes and is cooled by radiation. An additional cooling mechanism is due to decomposition of the dielectric material under high temperature. We will consider the situation where the thermal time constant is much shorter than the MP residual time. In this case, the MP has a uniform temperature throughout its volume and inward heat conduction from the surface may be neglected. The resulting energy balance reads

$$\frac{4}{3}\pi R_p^3 \rho C \frac{\mathrm{d}T_p}{\mathrm{d}t} = 4\pi R_p^2 (Q_{i,e} + Q_n - Q_r - Q_d) \tag{14}$$

According to the charging model (see Sec. II.B) the ion and electron fluxes are equal after the MP reaches steady-state charge. Therefore, the gross energy input by ions and electrons to the MP is given by the current density and the sum of the energy carried by each species:

$$Q_{i,e} = j_l(R_p)[2kT_e + kT_e + eU_p(t)] \tag{15}$$

where $U_p(t)$ is the time-dependent MP potential (see Sec. II.A).

The neutral atoms' heat transfer may be calculated using the Newtonian model

$$Q_n = \alpha \Delta T \tag{16}$$

In the general case, the coefficient of heat transfer is a complex function of MP size, gas flow temperature and velocity, heat conductivity, specific heat, and density. The relation between the coefficient of heat transfer and the preceding parameters was determined by a similarity law.[30] For the convective heat transfer between a body and gas flow, the following similarity can be used:

$$Nu = \alpha R_p / \lambda \tag{17}$$

Considering plasma–MP interaction in the PPT-4 cavity, one can estimate Nusselt number in the case when the particle is not moving relative to the plasma. In this case the Nusselt number Nu equals 2 (Ref. 30). The dependence of atomic thermal conductivity on temperature is given by: $\lambda = 2.4 \times 10^{-4} T^{3/4}$ W/mK (Ref. 30).

The radiative flux is given by the Stefan–Boltzmann law:

$$Q_r = \sigma_r \xi T^4 \tag{18}$$

The heat flux associated with material decomposition can be calculated as

$$Q_d = V_d \Delta H \tag{19}$$

The ablation rate can be estimated at equilibrium using Knudsen's law:

$$V_d = P_0 / \rho \sqrt{m_a / (2\pi kT)} \tag{20}$$

where P_0 is the equilibrium pressure of Teflon (see Refs. 1 and 4).

The rate of the MP radius change is determined by the ablation rate V_d:

$$\frac{\mathrm{d}R_p}{\mathrm{d}t} = -V_d \tag{21}$$

The initial condition is $R_p(t = 0) = R_{p0}$.

The calculated temporal variation of the MP temperature is shown in Fig. 7 with MP radius as a parameter. It can be seen that small MPs are heated substantially up to 1000 K during a short time period, whereas large MPs are only slightly affected by the plasma. Heating of the MP leads to significant ablation as plotted in Fig. 8. Note that small MPs (~1 μm) completely ablate if their residual time is larger than 0.5 μs.

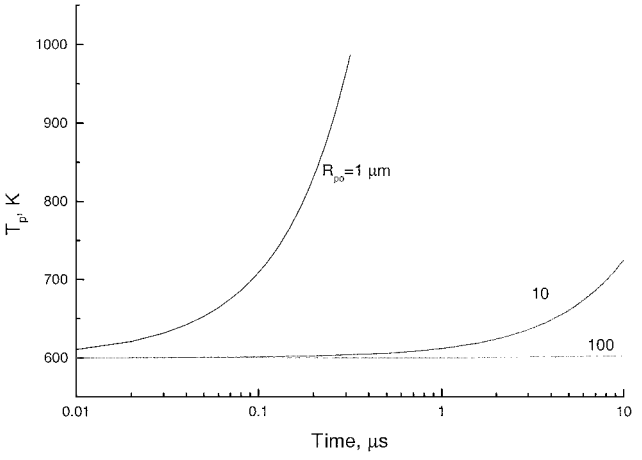

Fig. 7 Temporal dependence of the MP temperature with the MP radius as a parameter, T_e = 1.5 eV and $N = 10^{23}$ m^{-3}.

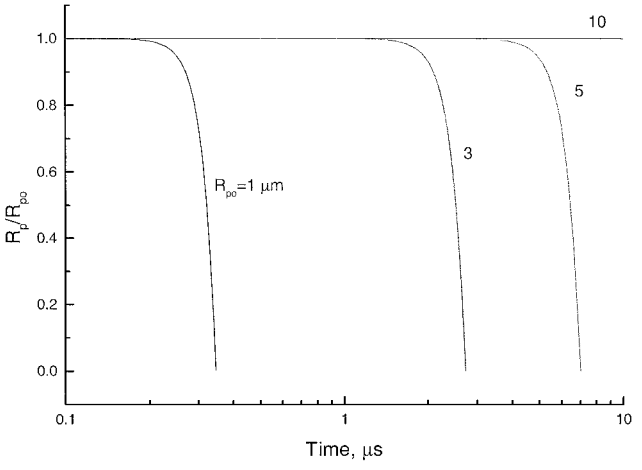

Fig. 8 MP radius vs time with the initial MP radius as a parameter, T_e = 1.5 eV and $N = 10^{23}$ m^{-3}.

III. Discussion

One of the important possible applications of the PPT is for attitude control of small satellites that are part of a group of close-flying satellites. In this case, interaction of the integrated plasma plume from the PPT with another spacecraft becomes an important issue. An experimental investigation has shown that the plasma plume contains a substantial fraction of MPs that originated from the dielectric as well as from the electrodes. The presence of such particles in the interacting plume may be a source of local damage to the spacecraft. The potential for MP damage on their collision with spacecraft surfaces depends on the MP directed velocity. The present calculation shows that the MP velocity depends mainly on MP size and residual time in the discharge. It was assumed that MP–plasma interaction occurs mainly during the discharge pulse. This is because the plasma density and temperature that control the interaction drop substantially after the pulse. Therefore, the maximum MP residual time considered in this model was equal to the pulse duration. Those small MPs emitted at the beginning of the discharge pulse may have a velocity of 200 m/s. Thus, one can expect a relatively broad range of MP velocity from zero up to a few hundred meters per second depending on the point of MP formation and the MP size. Another useful outcome from the MP velocity calculation is the possibility to estimate some characteristic time of MP flux ejection. Because MP velocity is generally smaller than the plasma velocity, and due to the broad range of MP velocities, the effective time of MP ejection from the thruster is much larger than the pulse duration. For instance, our estimation shows that the large MPs (~100 μm) exhaust from the thruster only after several seconds.

Because of the possible electrostatic nature of MP interaction with a spacecraft, the MP charge may play an important role. A spacecraft interacts with a plasma jet so as to become electrically charged to ensure zero net current, just like the MP. Thus, because the spacecraft has some negative potential with respect to the plasma, the MP may interact with the electric field in the thin sheath around the spacecraft. In some cases, the MP may be reflected in the sheath without mechanical collision with the surface. This effect has a positive role because the electrostatic nature of MP interaction with surfaces in space is not then connected with any mechanical damage. Thus, it is important to estimate the possibility of such MP–surface interactions. Previously, this effect was studied for the case of vacuum arc-generated MPs.[10,11] It was obtained both theoretically and experimentally for typical conditions that the electrostatic nature of the MP interaction with surfaces (without mechanical touching) is possible. It occurs in those cases when an MP approaches the surface with a grazing angle such that the MP kinetic energy will be smaller than the potential electrostatic energy. The possibility of this effect may be estimated using the following integral expression:

$$Q_p U_s > M_p V_{pn}^2 / 2$$

For instance, if the spacecraft potential U_s is about 10 V, a 1-μm MP may be electrostatically reflected if its normal velocity component is less than 4 m/s.

Another important outcome from the present study is prediction of the MP complete or partial decomposition due to interaction with the plasma during the discharge pulse. It was found that MPs with size less than 10 μm may totally decompose during 10 μs. However, large MPs may be still be present in the plasma plume. This means that the size distribution of MPs exhausted from the PPT is different from the original MP distribution. According to our calculation, the difference is more significant in the range of small MPs. Thus, any measurements of the MP flux in the plasma plume involve some combination of the original MP distribution and that from MP–plasma interaction rather than the size distribution of MPs emitted from the Teflon.[32] Note also that the MP decomposition may be a substantial volume source of the neutral component of the discharge plasma. However, because there is an uncertainty in the original MP size distribution, the significance of the last effect cannot be estimated accurately. One can also conclude that the increase in MP residence time leads to MP decomposition and, therefore, may have some effect on increasing propellant efficiency.

Note that in this paper the MP–plasma interaction was considered for the conditions typical for the electrothermal PPT-4 device. This device is fundamentally different from the usual LES 8/9 class PPT with dominant electromagnetic acceleration mechanism. It appears that the basic features of the present model should be same for electromagnetic PPT. The main difference is a much higher plasma velocity realized in this PPT due to $J \times B$ acceleration. It implies that the effective MP residual time may decreases, and, therefore, the MP charging, acceleration, and heating may be affected. Higher plasma velocity will increase the ion flux to the MP that may lead to increase MP charge in the steady state. However, because the MP steady-state charge depends logarithmically on the ion flux, one would expect only small changes. Small (submicrometer) MPs have the potential for acceleration when they interact with a high-velocity plasma jet.

IV. Conclusion

We have shown that the plasma may affect particulate contamination from the plume of a PPT. During flight, a MP may become charged, heated, and accelerated. It was found that the charging time depends on MP size and is generally smaller in the case of small MPs. We have found that a 1-μm MP has a charge of about 10^5 electrons in the case of an electron density of about 10^{23} m^{-3}. There are two primary forces acting on the MP in the PPT discharge: a drag force due to collision with neutral atoms and ions and an electric force due to the presence of the electric field in a current carrying plasma. The maximum possible velocity of a 1-μm MP is about 230 m/s, which is close to that estimated experimentally. Only small

MPs ($\sim$0.1 μm) can be entrained by the plasma jet, whereas large MPs are generally slower and flow substantially behind the plasma jet. Small MPs ($<$1 μm) may completely decompose during a 1-μs pulse.

Acknowledgments

This work was supported by the Air Force Office of Scientific Research through Grant F49620-99-1-0040. The authors acknowledge R. Burton and S. Bushman from the University of Illinois, Urbana–Champaign, for valuable discussions and for providing experimental data prior to publication.

References

[1]Burton, R. L., and Turchi, P. J., "Pulsed Plasma Thruster," *Journal of Propulsion and Power*, Vol. 14, No. 5, 1998, pp. 716–735.

[2]Spores, R. A., Cohen R. B., and Birkan, M., "The USAF Electric Propulsion Program," *Proceedings of the 25th International Electrical Propulsion Conference*, Electric Rocket Propulsion Society, Worthington, OH, 1997, pp. 1–8.

[3]Vondra, R. J., "The MIT Lincoln Laboratory Pulsed Plasma Thruster," AIAA Paper 76-998, July 1976.

[4]Mikellindes, P. G., and Turchi, P. J., "Modeling of Late-Time Ablation in Teflon Pulsed Plasma Thruster," AIAA Paper 96-2733, July 1996.

[5]Spanjers, G. G., Lotspeich, J. S., McFall, K. A., and Spores, R. A., "Propellant Losses Because of Particulate Emission in a Pulsed Plasma Thruster," *Journal of Propulsion and Power*, Vol. 14, No. 4, 1998, pp. 554–559.

[6]Roth, R. M., Spears, K. G., Stein, G. D., and Wong, G., "Spatial Dependence of Particle Light Scattering in an of Silence Discharge," "Spatial Dependence of Particle Light Scattering in an rf Silane Discharge," *Applied Physics Letters*, Vol. 46, No. 3, 1985, pp. 253–255.

[7]Hwang, H., Keiter, E. R., and Kushner, M. J., "Consequences of Three-Dimensional Physical and Electromagnetic Structures on Dust Particle Trapping in High Plasma Density Material Processing Discharges," *Journal Vacuum Science Technology*, Vol. A 16, No. 4, 1998, p. 2454.

[8]Selwyn, G. S., Heidenreich, J. E., and Haller, K. L., "Particle Trapping Phenomena in Radio Frequency Plasmas," *Applied Physics Letters*, Vol. 57, No. 18, 1990, pp. 1876–1878.

[9]Barnes, M. S., Keller, J. H., Forster, J. C., O'Neil, J. A., and Coultas, D. K., "Transport of Dust Particles in Glow-Discharge Plasmas," *Physical Review Letters*, Vol. 68, No. 3, 1992, pp. 313–316.

[10]Keidar, M., Beilis, I. I., Boxman, R. L., and Goldsmith, S., "Transport of Macroparticles in Magnetized Plasma Ducts," *IEEE Transactions on Plasma Science*, Vol. 26, No. 2, 1996, pp. 226–234.

[11]Keidar, M., Beilis, I. I., Aharonov, Arbilly, R. D., Boxman, R. L., and Goldsmith, S., "Macroparticle Distribution in a Quarter-Torus Plasma Duct of a Filtered Vacuum Arc Deposition System," *Journal Physics D: Applied Physics*, Vol. 30, Nov. 1997, pp. 2972–2978.

[12]Gatsonis, N. A., Erlandson, R. E., and Meng, C. I., "Simulation of Dusty Plasmas Near Surfaces in Space," *Journal of Geophysical Research*, Vol. 99, No. A5, 1994, pp. 8479–8489.

[13]Aleksandrov, V. V., Belan, N. V., Koslov, N. P., Mashtylev, N. A., Popov, G. A., and Khvesiyk, V. I., "Pulse Plasma Accelerators," KHAI, Kharkov, 1983 (in Russian), p. 55.

[14]Boxman, R. L., Martin, P. J., and Sanders, D. (eds.), *Handbook of the Vacuum Arc Science and Technology*, Noyes, Park Ridge, NJ, pp. 1995.

[15]Vladimirov, V. V., Badan, V. E., and Gorshkov, V. N., "Microdroplet Emission and Instabilities in Liquid-Metal Ion Sources," *Surface Science*, Vol. 266, April 1992, p. 185.

[16]Parkus, H., *Thermoelasticity*, Blaisdell, Waltham, MA, 1968, pp. 70–100.

[17]Turchi, P. J., "Direction for Improving PPT Performance," *Proceedings of the 25th International Electrical Propulsion Conference*, Electric Rocket Propulsion Society, Worthington, OH, 1997, pp. 251–258.

[18]Ogurtsova, N. N., Podmoshenskii, I. V., and Rogovtsev, P. N., "Calculation of the Parameters of an Optically Dense Plasma Obtained by a Discharge with an Evaporating Wall," *High Temperature*, Vol. 9, 1971, pp. 430–436.

[19]Burton, R. L., Hilko, B. K., Witherspoon, F. D., and Jaafari, G., "Energy-Mass Coupling in High-Pressure Liquid-Injected Arcs," *IEEE Transactions on Plasma Science*, Vol. 19, No. 2, 1991, pp. 340–349.

[20]Bushman, S. S., "Investigation of a Coaxial Pulsed Plasma Thruster," M.S. Thesis, Univ. of Illinois, Urbana–Champaign, IL, May 1999.

[21]Kilgore, M. D., Daugherty, J. E., Porteous, R. K., and Graves, D. B., "Ion Drag on an Isolated Particulate in a Low-Pressure Discharge," *Journal Applied Physics*, Vol. 73, No. 11, 1993, pp. 7195–7202.

[22]Keidar, M., Beilis, I. I., Boxman, R. L., and Goldsmith, S., "Non-Stationary Macroparticle Charging in an Arc Plasma Jet," *IEEE Transactions on Plasma Science*, Vol. 25, No. 6, 1995, pp. 902–908.

[23]Mott-Smith, H. M., and Langmuir, I., "Collectors in the Gaseous Discharges," *Physics Review*, Vol. 28, 1926, p. 727.

[24]Laframboise, J. G., and Parker, L. W., "Probe Design for Orbit-Limited Current Collection," *Physics of Fluids*, Vol. 16, No. 5, 1973, pp. 629–636.

[25]Swift, J. W., and Schwar, M. J. R., *Electrical Probes for Plasma Diagnostics*, Iliffe, London, 1970.

[26]Whipple, E. C., "Potential of Surfaces in Space," *Reports on Progress in Physics*, Vol. 44, 1981, pp. 1197–1250.

[27]Kilgore, M. D., Daugherty, J. E., Porteous, R. K., and Graves, D. B., "Transport and Heating of Small Particles in High Density Plasma Sources," *Journal Vacuum Science and Technology*, Vol. B 12, No. 1, 1994, pp. 486–493.

[28]Boxman, R. L., and Goldsmith, S., "The Interaction Between Plasma and Macroparticles in a Multi-Cathode Spot Vacuum Arc," *Journal of Applied Physics*, Vol. 52, No. 1, 1981, pp. 151–161.

[29]Baines, M. J., Williams, I. P., and Asebiomo, A. S., "Resistance to the Motion of a Small Sphere Moving Through a Gas," *Monthly Notices of the Royal Astronomical Society*, Vol. 130, Sept. 1965, pp. 63–74.

[30]Dresvin, S. V. (ed.), *Physics and Technology of Low-Temperature Plasmas*, Iowa State Univ. Press, Ames, IA, 1977.

[31]Crowe, C. T., "Drag Coefficient of Particles in a Rocket Nozzle," *AIAA Journal*, Vol. 5, May 1967, pp. 1021, 1022.

[32]Newman, R. L., "A Kinetic Treamment of Ablation," *Journal of Spacecraft*, Vol. 3, May–June 1965, pp. 450, 451.